Available online at www.sciencedirect.com

SciVerse ScienceDirect

Journal of the European Ceramic Society 32 (2012) 1625–1634

www.elsevier.com/locate/jeurceramsoc

Stereolithography process: Influence of the rheology of silica suspensions and of the medium on polymerization kinetics – Cured depth and width

T. Chartier [a,*], A. Badev [a], Y. Abouliatim [a], P. Lebaudy [b], L. Lecamp [b]

[a] SPCTS – UMR CNRS 6638, Centre Européen de la Céramique, 12, rue Atlantis, 87068 Limoges Cedex, France
[b] INSA de Rouen, UMR CNRS 6270, PBS, FR CNRS 3038, Avenue de l'Université, BP 08, 76801 Saint Etienne du Rouvray Cedex, France

Received 8 September 2011; received in revised form 21 December 2011; accepted 7 January 2012
Available online 2 February 2012

Abstract

UV laser stereolithography is a rather new shaping technique that makes it possible the fabrication of complex 3D ceramic structures with a high dimensional accuracy. The green part is built through layer by layer photopolymerization of a light sensitive suspension.

Polymerization is thus a critical step to control in this shaping technique. Photopolymerization, with the initiation, propagation and termination reactions, involves the mobility of reactive species and is then sensible to the rheology of the media. This study investigated the influence of the rheology of suspensions of silica particles in an acrylate oligomer and of the intergranular curable organic phase on the UV polymerization. In this respect, the effects of the powder concentration, the state of dispersion and of the dilution of the reactive oligomer on polymerization, are measured.

In addition, the influence of the powder loading on the cure depth and cure width, which are respectively pertinent indicators of the reactivity of the suspension and of the dimensional accuracy of the green part, is evaluated.

Keywords: Suspensions; Sintering; SiO_2; Shaping

1. Introduction

Stereolithography (SL) is a rapid prototyping process that opens the possibility to fabricate complex 3D functional ceramic components without tooling and with a good dimensional resolution.[1–3] This technology is based on the photopolymerization, by a UV laser beam, of a curable system consisting of a dispersion of ceramic particles in a sensitive monomer/oligomer resin.[4] The polymerization of cross sectional sections of successive layers of a part leads to the creation of sophisticated 3D objects, that are physically built by an automated machine which uses the three dimensional CAD file of the part to be built. This rather recent fabrication technique has found numerous applications in different fields among them, microelectronics with the production of microwave devices (filters, resonators)[5–7] with a high dimensional accuracy or biological domain with hydroxyapatite implants.[8]

The objective of this study is to evaluate the respective contribution of the rheology of suspensions containing ceramic particles and of the rheology of the intergranular reactive phase on the photopolymerization (measurement of the kinetics of conversion and of the conversion rate). Silica, with a refractive index close to that of the resin, was chosen as ceramic material. In this respect, different parameters such as the powder loading, the state of dispersion, varying the addition of a dispersant and the addition of a diluent, were used to change the rheology of the suspension and of the viscosity of the intergranular reactive phase. Finally, the influence of the powder concentration on key parameters in terms of UV reactivity of the system and of dimensional resolution (i.e. polymerized thickness (E_p) and polymerized width (L_p)) were evaluated.

2. Experimental procedure

2.1. Staring materials

The ceramic material used is a silica powder (Cerac, USA) with a specific area of 5.31 m^2 g, a refractive index of 1.564 and

* Corresponding author. Tel.: +33 (0)5 87 50 23 10.
E-mail address: thierry.chartier@unilim.fr (T. Chartier).

0955-2219/$ – see front matter © 2012 Elsevier Ltd. All rights reserved.
doi:10.1016/j.jeurceramsoc.2012.01.010

a mean particle size of 2.25 μm (d_{50}). In order to improve its dispersion in the UV curable suspension and the homogeneity of the microstructure of the green part, the as received silica powder is deagglomerated by attrition milling using 1 mm diameter zirconia balls. This deagglomeration is performed during 4 h in ethanol with the addition of 0.5 wt% (on the dry powder basis) of one phosphate ester (PE) as dispersant.

The UV curable system is composed of a photoinitiator dissolved in a reactive amine modified polyester acrylate (PEAAM) with a density of 1.15 g cm^{-3} and a refractive index of 1.488. The photoinitiator is a phenylacetophenone derivative (2,2-dimethoxy-1,2-phenylacetophenone DMPA, Ciba, France) which absorbs in the range of 220–380 nm. A reactive diluent (1,6 hexanediol diacrylate – HDDA – density = 1.02 g cm^{-3}, refractive index = 1.456) has been added in order to improve the flow behavior of the suspensions, due to its low viscosity (8.3 mPa s at 20 °C). HDDA presents a good miscibility with the PEAAM oligomer.

2.2. Preparation and characterization of the UV-curable suspensions

The photoinitiator and the dispersant were first introduced in the PEAAM oligomer by stirring the mixture during 4 h in the dark. The ceramic powder was then incorporated into the organic mixture and kneaded in order to eliminate residual agglomerates and thus to obtain a good homogeneity.

Rheological measurements of the suspensions were performed with a controlled stress rheometer using a cone-plane configuration (50 mm cone diameter, 1.59° angle and truncation of 49 μm). The rheological behavior of the suspensions was analyzed using Hershel–Bulkley model for nonlinear behavior of these heterogeneous systems:

$$\tau = \tau_0 + K \cdot \gamma^n \quad (1)$$

where τ (N m^{-2}) is the shear stress, γ (s^{-1}) the shear rate, τ_0 (N m^{-2}) the yield stress, n the shear rate exponent ($n = 1$ for Newtonian fluid) and K a constant.

2.3. Curing of the ceramic suspensions

The stereolithography process is based on the space resolved photopolymerization of a reactive suspension into a solid green part. Following a chemical reaction induced by absorption of radiation, the photoinitiator releases reactive species, initiating the polymerization reaction that makes it possible the transformation of the liquid monomer/oligomer into solid polymer.[9]

During the construction of the object, the working plate is immersed in the tank filled with the curable system, at a depth equal to the thickness of one layer. The layer thickness is adjusted by spreading the suspension with a blade. The laser beam scans the surface of the resin, point by point, following CAD guidelines, providing a localized polymerization (solidification) of irradiated cross-sectional areas. After completion of one layer, the working plate moves down to a layer thickness and the process is repeated until all cross-sections of the object to be built

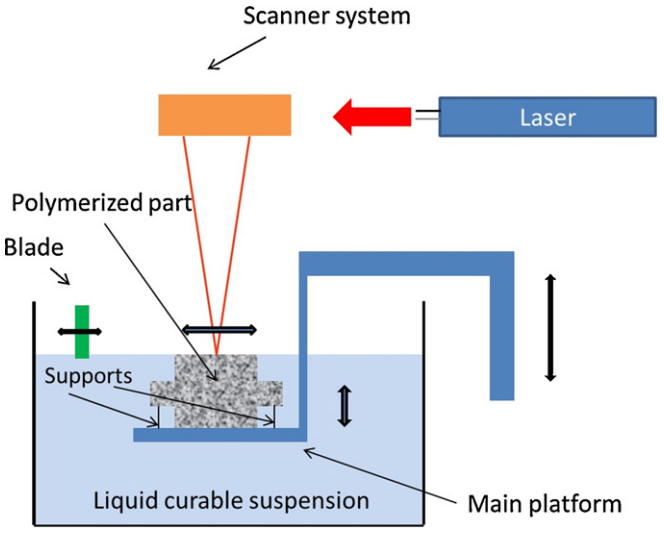

Fig. 1. Principle of the stereolithography process.

are solidified (Fig. 1). The object is then extracted from the tank and the uncured suspension is removed using an appropriate solvent. The resolution of the method is of 100 μm.

The key parameters, in terms of UV reactivity of the system and of dimensional resolution, which are the polymerized thickness (E_p) and width (L_p) are measured. A thick film (2–3 mm) of the suspension is manually spread onto the fabrication plate. This large thickness avoids the polymerized lines to stick to the support. A series of 40 parallel lines, 10 mm length and 1 mm spaced were polymerized by laser scanning, thus drawing a 10 mm × 40 mm rectangle (Fig. 2a). After photopolymerization, the rectangle is washed out of the residual non polymerized suspension by a solvent, then coated with a transparent resin, and finally cut perpendicular to its length. A total number of 40 filaments have been recovered (Fig. 2b). The line profiles were observed and the measurements of E_p and L_p were performed using an optical microscope equipped with a digital camera and a software. The error on the determination of E_p and L_p is evaluated to be few microns.

UV curing was performed with a 353 nm wavelength argon ionized laser with a maximum output power of 1 W. The

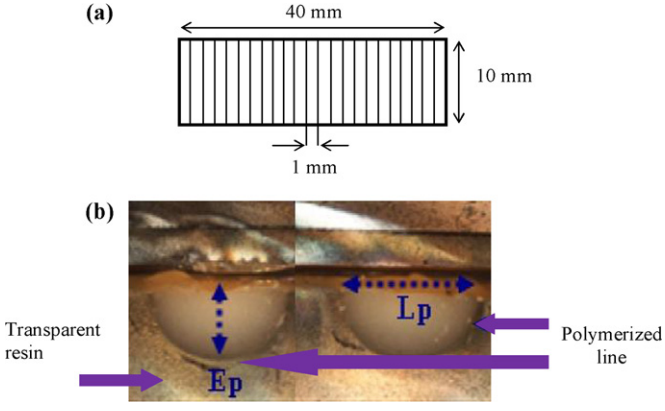

Fig. 2. (a) Shape configuration containing the polymerized lines. (b) Examples of profile sections of two polymerized lines.

projected density of energy E_i (mJ cm^{-2}) is related to the nominal laser power (P_0), scanning speed (v_s) and beam radius (ω_0) through the following equation:

$$E_i = \frac{2P_0}{\pi\omega_0 v_s} \quad (2)$$

The scanning speed is specified in the program that controls the stereolithography process. The radius of the laser spot in the focal plane is 100 μm (estimated experimentally) and the output power is measured by a wattmeter. These parameters are considered constant during the scanning process that leads to practically identical polymerized line sections.

2.4. Photopolymerization of acrylate resins

Photopolymerization is a chain of reactions and its initiation stage is of photochemical nature. Multifunctional monomers/oligomers lead to a dense crosslinked 3D network upon curing. Radical photopolymerization is the most used reaction for stereolithography applications. It takes place within the curing of high UV reactivity monomers/oligomers having a vinyl unsaturation, such as acrylates and methacrylates. Their nature impacts the final properties of the reticulated polymer: elastic and opaque in case of acrylates; hard and transparent in case of methacrylates. Due to the faster cure response of acrylates, the liquid to solid phase change is immediate (~0.2 s) upon intense radiation.[10,11] The group of polyester acrylates encloses a large variety of low viscosity oligomers with different functionalities and molar masses (such as PEAAM resin used in this study).

The radical photopolymerization process of polyester acrylates occurs in three stages: initiation, propagation and termination.

2.4.1. Initiation

The first stage of the reaction corresponds to the initiation, i.e. the activation of a monomer/oligomer molecule by the photoinitiator (PA). The photopolymerization undergoes its decomposition (PA*) under the influence of UV irradiation in order to generate two free radicals R°_1 and R°_2 following the reaction:

$$PA \xrightarrow{h\nu} PA^* \rightarrow R_1^{\circ} + R_2^{\circ} \quad (3)$$

One or both radicals will combine with a molecule of the monomer/oligomer (M), and therefore generates a new radical RM, able to propagate the polymerization reaction as follows:

$$R^{\circ} + M \rightarrow RM^{\circ} \quad (4)$$

The rate of initiation v_a is directly related to the quantum yield of initiation ϕ_a and to the absorbed radiation intensity I_{abs}.

$$v_a = \phi_a \cdot I_{abs} \quad (5)$$

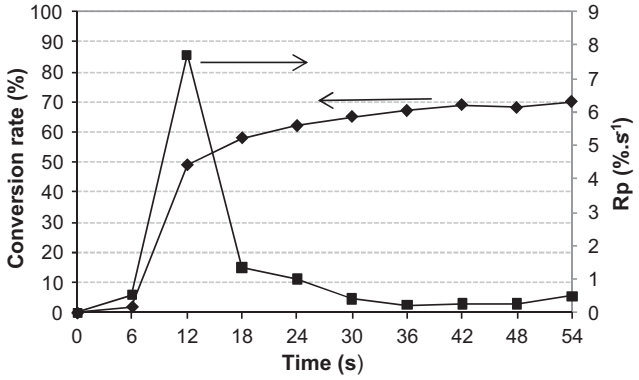

Fig. 3. Conversion and rate of polymerization (Rp) for PEAAM + 0.5 wt% photoinitiator for an energy doze of 5.3 mW cm^{-2}.

2.4.2. Propagation

This stage corresponds to the successive addition of monomer/oligomer units on the growing polymer chain, in order to generate larger radicals:

$$RM_n^{\circ} + M \xrightarrow{k_p} RM_{n+1}^{\circ} \quad (6)$$

The rate of propagation v_b, reflecting the variation of the monomer/oligomer concentration [M], along the reaction is:

$$v_p = k_p[RM_n^{\circ}] \cdot [M] \quad (7)$$

where k_p is the propagation rate constant.

The kinetics of the photopolymerization reaction of multifunctional acrylates shows a particular behavior: self-acceleration and self-deceleration phenomena accompanied by an incomplete conversion of functional groups.[11]

2.4.3. Termination

The termination corresponds to the end of the photopolymerization process, i.e. the end of the chain growth. The rate of termination v_t is expressed by:

$$v_t = k_t[RM_n^{\circ}] \quad (8)$$

where k_t is the termination rate constant.

The technique used to determine the degree of the reaction, respectively the rate of conversion, of an acrylate double bond is Real-Time Infrared Spectroscopy (RTIR). This technique, described elsewhere is based on the variation in absorption of reactive functions at each time of the reaction.[12–14] The degree of conversion is determined by the rate of polymerization (Rp) during photopolymerization of a monomer/oligomer. The rate of polymerization can be considered as the rate of disappearance of monomer with respect to time, $-d[M]/dt$.

The conversion and the rate of polymerization (Rp) of a UV sensible medium are governed by the propagation (k_p) and termination (k_t) constants. Two main stages take place: at first, the irradiation of the monomer/oligomer leads to a rapid increase of the polymerization rate (Rp) that reaches its maximum, and corresponds to a conversion of about 50% (Fig. 3). This is the stage of self-acceleration or Trommsdorff effect that leads to the formation of a gel at the beginning of the polymerization. The

mobility of reactive species is then very limited in the medium, and the termination reaction is also limited. Rp is then decreasing as the viscosity continues to increase with a lower mobility of free radicals. Kp and Rp are decreasing, thus the propagation constant is controlled by the diffusion reaction. This is the self-deceleration stage. The intermolecular Wan Der Waals bonds convert to intramollecular covalent bonds. This generates a free volume where the mobility of reactive species is larger and contributes to a further increase of the conversion rate at the end of the reaction. Indeed, the propagation and termination reactions (k_p and k_t) are conditioned by the diffusion of reactive species in the medium which tends to a vitreous state.

At the end of the photopolymerization reaction, the % conversion is lower than 100%.

3. Results and discussions

3.1. Rheological behavior of the ceramic suspensions

The introduction of ceramic particles in a curable resin will drastically modify its rheological behavior. The increase in viscosity will depend on the nature (surface chemistry), the concentration, the shape and the size distribution of ceramic particles. The overall viscosity is increasing at a macroscopic level with the powder loading, but the viscosity of the intergranular organic phase may be not affected by the presence of ceramic particles.

In presence of a volume fraction Φ of ceramic powder, the increase of the viscosity can be evaluated by the Krieger–Dougherty equation:

$$\eta_r = \frac{\eta}{\eta_0} = \left(1 - \frac{\beta.\Phi}{\Phi_0}\right)^{-[\eta]\Phi_0} \quad (9)$$

where η_r is the relative viscosity of the resin, η is the viscosity of the suspension at a very low shear rate, η_0 is the viscosity of the organic medium, Φ_0 the volume fraction of the filler for a close-packed particles corresponding to an infinite viscosity (no flow) and $[\eta]$ the intrinsic viscosity which depends on the shape of particles ($\eta = 2.5$ for spheres).

The reaction of photopolymerization is essentially controlled by diffusion mechanisms directly linked to the evolution of the viscosity during curing. At the beginning of the photopolymerization, the viscosity of the curable system rapidly increases, and then continues to increase during all the reaction of photopolymerization. This generates a "resistance" to the diffusion of the various reactive species involving in the propagation reaction (mobility of the reactive species) and in the termination reaction (mobility of radical sites developing the network).

Indeed, the evolution of the viscosity of a loaded system, during polymerization, will directly influence the "diffusional capacity" of reactive species and more precisely their allowed distance of mobility. For instance, at high powder concentration with a small interparticle distance, some steps of propagation are sufficient to interconnect particles dispersed in the polymeric network. That accelerates the increase of viscosity of the reactive system and may influence the further polymerization reactions of propagation and termination.

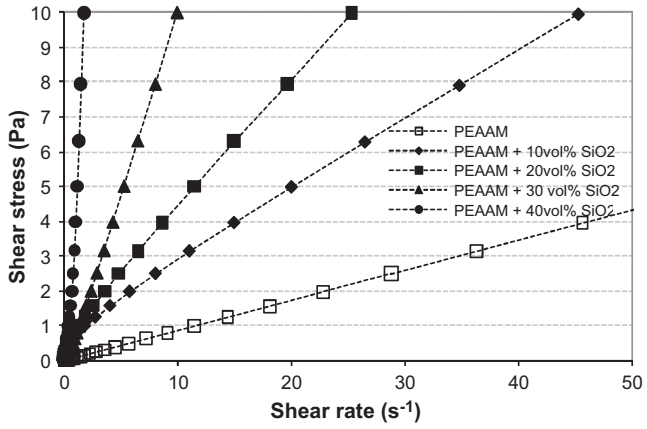

Fig. 4. Flow curves, at 20 °C, of PEAAM oligomer and of suspensions loaded with 10–40 vol% SiO_2 + 0.5 wt% phosphate ester (PE) dispersant.

In this context, we will evaluate the respective contribution of the rheology of the curable suspension and of the rheology of the intergranular resin on the photopolymerization of loaded silica suspensions.

3.1.1. Influence of the ceramic concentration

The oligomer used (PEAAM) presents a Newtonian behavior with an apparent viscosity of 84 mPa s (Fig. 4). The photoinitiator was found to have no effect on the rheology of the resin, and whatever its concentration, the resin exhibits a Newtonian behavior. With the incorporation of silica particles and a dispersant PE (0.5 wt%), Hershel–Bulkley model (Table 1) reveals a shear-thinning behavior ($n < 1$) for concentrations below 20 vol% of silica loading, and a shear-thickening behavior for larger powder concentrations. The yield stress is low and below the uncertainty of modeling.

In the case of this transparent filler (silica) with a low refractive index difference with PEAAM resin, the kinetics of polymerization of suspensions containing 10 vol% of silica is identical to that of the pure PEAAM (Fig. 5a), despite the important change of viscosity (Fig. 4). That suggests that the rheology of low concentrated systems does not influence the diffusional mechanisms during photopolymerization. For 10 vol% silica, the distance between particles, estimated from a cubic-centered arrangement of 2.25 μm diameter spheres, is 1.67 μm. We can thus consider that this value represent an upper limit of the implicated distance in the diffusional mechanisms. The rheological changes induced by the higher particle–monomer and particle–particle interactions, for powder concentrations above 10 vol%, decrease the % conversion of the suspensions as well as the polymerization rate (Fig. 5b) due to a lower diffusional capacity of the reactive species. The overall viscosity increases at a macroscopic state, and the viscosity of the intergranular phase remains unchanged.

At larger powder loading (>10 vol%), the challenge is to change the overall rheology of the suspension, for a given powder concentration, without altering the photosensitive matrix, and then to preserve the same reactivity and rheology of the intergranular phase (organic medium). In this respect, we have modified the state of dispersion of silica particles in the organic

Table 1
Hershel–Bulkley parameters, viscosity at a low shear rate, relative viscosity (η_r), and maximum rate of polymerization measurements (Rp max) of PEAAM resin and silica loaded suspensions (10–40 vol%) with the addition of 0.5 wt% PE.

Composition	$\eta_{(\text{low shear rate})}$ (Pa s)	n	η_r	Rp max (% s^{-1})	K
PEAAM	0.084	1	1	5.93	$K = \eta = 0.084$
PEAAM + 10 vol% SiO_2 + 0.5 wt% PE	0.21	0.81	2.5	5.25	0.43
PEAAM + 20 vol% SiO_2 + 0.5 wt% PE	0.37	0.83	4.4	4.62	0.65
PEAAM + 30 vol% SiO_2 + 0.5 wt% PE	1.04	1.11	12.38	4.05	0.78
PEAAM + 40 vol% SiO_2 + 0.5 wt% PE	1.48	2.00	17.62	2.45	2.60

phase by varying the concentration of the phosphate ester (PE) dispersant. We have previously verified that the addition of PE dispersant has no significant effect on the viscosity of the PEAAM resin.

3.1.2. Influence of the rheology of the suspension (addition of a dispersant)

Slurries containing 40 vol% of silica were prepared with different concentrations of dispersant (1–5 wt% with respect to the powder) leading to an important modification of the suspension rheology (Fig. 6). As the addition of PE dispersant does not influence the viscosity of the PEAAM resin, we can assume that the viscosity of the intergranular phase was unchanged. In case of a perfect dispersion (independent grains), the distance between particles (estimated by the previously mentioned method) is 0.21 μm, which is 8 times smaller than the one for a suspension loaded with 10 vol% of silica.

The shear-thickening behavior becomes more pronounced with the increase of the dispersant concentration (Table 2). Nevertheless, as the photopolymerization takes place when the suspension is at rest, without shearing, the shear-thickening character cannot be retained as a pertinent indicator of the modification of the global rheology of the various suspensions. On the contrary, the viscosity at very low share rate, estimated from the flow curves tangent (Fig. 6) can be considered as a pertinent characteristic of the suspension during UV polymerization. The increase of the viscosity at rest with the concentration of dispersant is likely due to an increase of interactions between adsorbed chains of dispersant onto the particle surfaces.

Whatever the concentration of dispersant, then the rheology of the suspension, the conversion profiles at late reaction are similar for all compositions (Fig. 7a). The conversion at maximum polymerization rate changes from 42% for the composition containing 1 wt% PE, to 26% for compositions containing larger concentrations of PE (Fig. 7b). As Rp is proportional to $(Kp/Kt)^{0.5}$, and considering the similarity of the conversion profiles after 60 s, the rheological changes induced by the adsorbed dispersant–dispersant chain interactions influence the propagation rate (decrease of Kp). This suggests that the relative viscosity of the suspension affects the early stage of the photopolymerization process as shown in Fig. 7c.

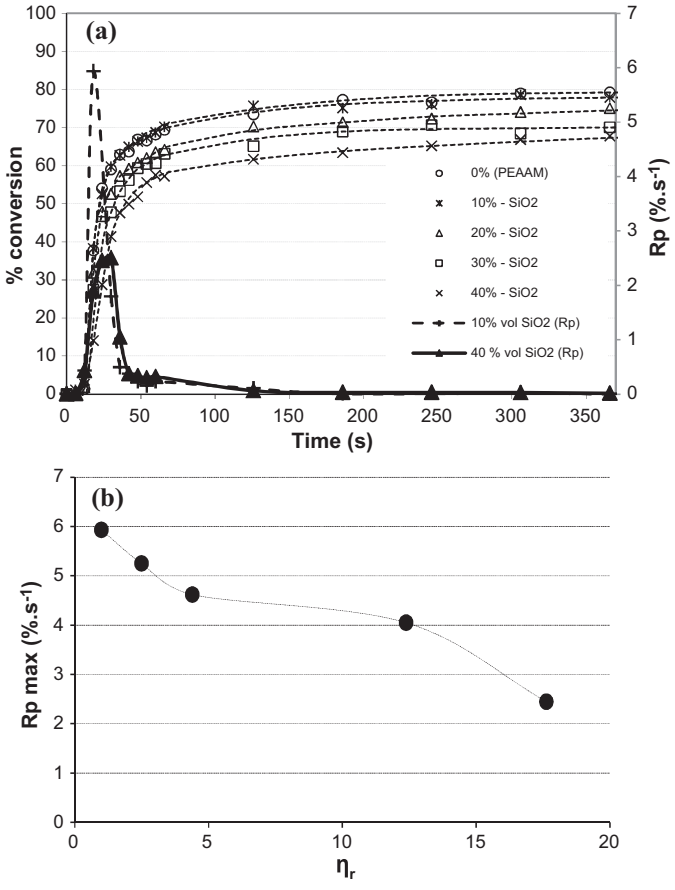

Fig. 5. PEAAM + 0.5 wt% photoinitiator under an energy doze of 5.3 mW cm^{-2} for different silica concentrations. (a) Conversion and polymerization rate versus time; (b) maximum rate of polymerization versus relative viscosity.

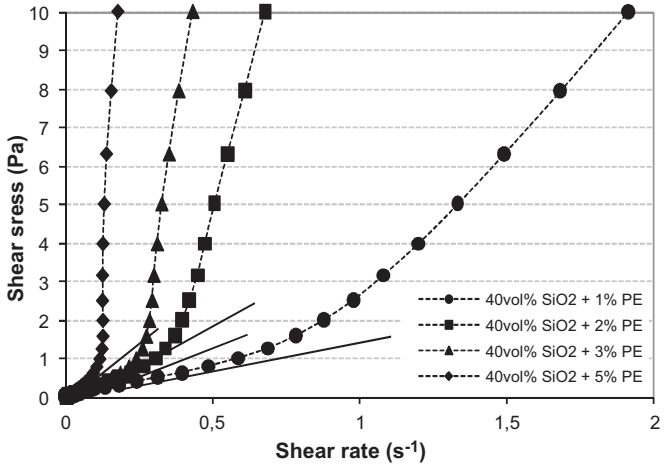

Fig. 6. Flow curves, at 20 °C, of 40 vol% loaded PEAAM suspensions containing 1–5 wt% phosphate ester (PE) dispersant.

Table 2
Hershel–Bulkley parameters, viscosity at a low shear rate, relative viscosity (η_r), and maximum rate of polymerization measurements (Rp max), for 40 vol% silica suspensions loaded with different PE dispersant concentrations.

Composition	η (low shear rate) (Pa s)	n	η_r	Rp max (% s^{-1})	K
PEAAM + 40 vol% SiO_2 + 1 wt% PE	1.65	2.04	19.64	4.09	2.7
PEAAM + 40 vol% SiO_2 + 2 wt% PE	2.95	2.82	35.12	3.85	30.8
PEAAM + 40 vol% SiO_2 + 3 wt% PE	4.05	3.40	48.21	3.05	186.2
PEAAM + 40 vol% SiO_2 + 5 wt% PE	6.20	3.81	73.8	2.66	7832

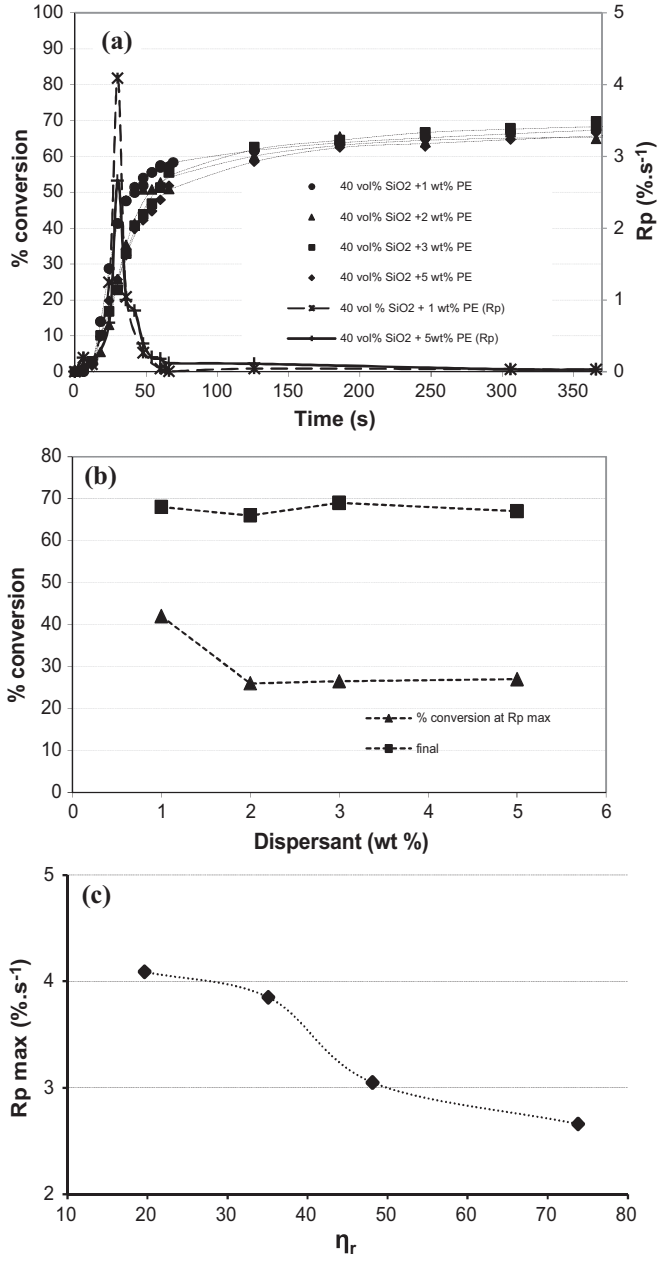

Fig. 7. Effect of the rheology on the polymerization of 40 vol% silica loaded suspensions containing different concentrations of dispersant (PE), under an energy doze of 5.3 mW cm^{-2}. (a) Conversion and polymerization rate versus time, (b) conversion at maximum polymerization rate and at the end of the reaction, and (c) maximum polymerization rate versus relative viscosity.

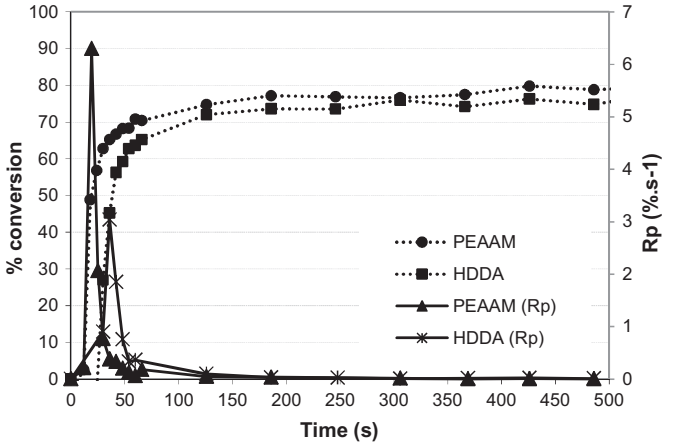

Fig. 8. Conversion and rate of polymerization (Rp) of PEAAM oligomer and HDDA monomer.

3.1.3. *Influence of the rheology of the intergranular reactive phase (addition of a diluent)*

Various studies have shown that the decrease of the viscosity of the reactive organic phase is beneficial to the reaction of photopolymerization.[9,12,13] An acceleration of the reaction of photopolymerization is attributed to a better mobility of reactive radicals. In this respect, we have evaluated the influence of the decrease of the viscosity of PEAAM, by addition of a diluent, on the photopolymerization.

The diluent chosen is a bi-functional acrylate monomer used in classic curable formulations: 1,6 hexanediol diacrylate (HDDA). Its viscosity (8.3 mPa s at 20 °C) is 10 times lower than that of PEAAM and has similar reactive functions (acrylate functions) than those of PEAAM oligomer. As the reactive diluent changes the viscosity of the medium, it also affects the reaction rate (Rp), since PEAAM oligomer and HDDA monomer have different polymerization rates, as shown in Fig. 8:

Concentrations from 10 to 25 vol% of HDDA monomer were introduced in substitution to PEAAM oligomer. The concentration of photoinitiator remains 0.5 wt% on the (PEAAM + HDDA) basis. All compositions exhibit a Newtonian behavior and the viscosity is considerably decreasing with HDDA addition (Table 3).

A concentration of HDDA comprised between 10 and 25 vol% in PEAAM–HDDA mixtures led to a maximum % conversion (Fig. 9). In this respect, suspensions containing 40 vol% silica particles into a PEAAM–HDDA reactive mixture containing 10 and 25 vol% HDDA were prepared to evaluate the influence of the mobility of reactive functions in a concentrated system.

Table 3
Hershel–Bulkley parameters, viscosity at a low shear rate, relative viscosity (η_r), and maximum rate of polymerization measurements (Rp max), for PEAAM/HDDA suspensions loaded with 40 vol% silica (1 wt% PE).

Organic composition 40 vol% SiO_2 + 1 wt% PE	η (low shear rate) (Pa s)	n	K	$\eta_{(organic\ medium)}$ (Pa s)	η_r	Rp max (% s^{-1})
PEAAM	1.65	2.04	2.67	0.084	19.64	2.46
PEAAM + 10 vol% HDDA	1.71	1.90	2.80	0.060	26.37	3.05
PEAAM + 25 vol% HDDA	1.26	1.50	1.69	0.038	32.98	2.64

The addition of HDDA up to about 10 vol% does not considerably change the viscosity of suspensions containing 40 vol% silica (Fig. 10, Table 3). Nevertheless, for an addition of 10 vol% HDDA, an increase of the polymerization rate and of the final conversion is observed (Fig. 11a and b) that is likely due to the generation of a free volume in the organic medium where the mobility of reactive species is larger, thus leading to a higher degree of conversion at the end of the reaction and higher polymerization rates than the pure PEAAM 40 vol% silica filled suspension (Fig. 11b).

For suspensions having the same concentration of ceramic particles, only the viscosity of the intergranular phase can be

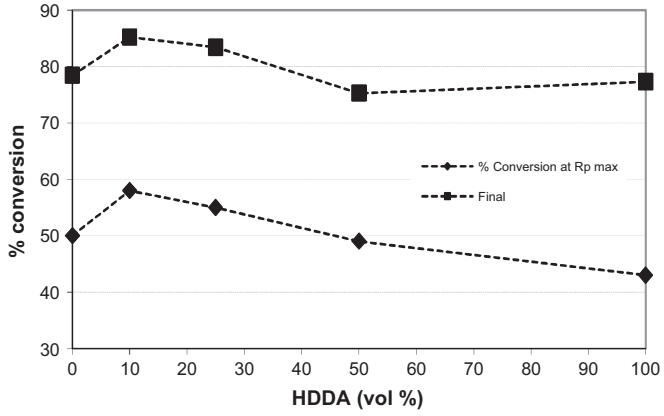

Fig. 9. Influence of the addition of HDDA monomer in PEAAM oligomer on the polymerization of the PEAAM–HDDA mixtures for an energy doze of 5.3 mW cm^{-2}.

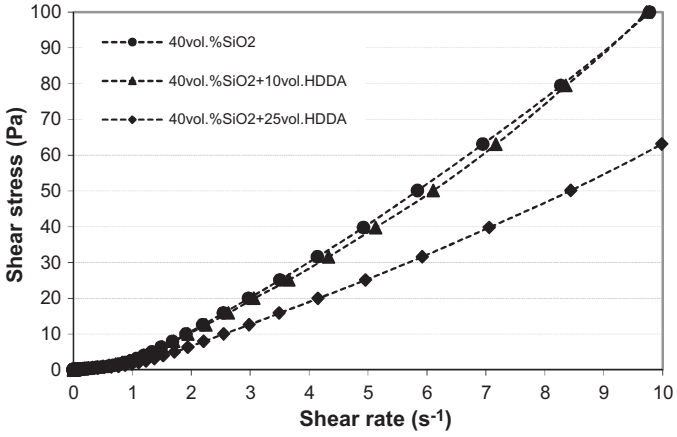

Fig. 10. Flow curves at 20 °C of 40 vol% silica loaded PEAAM/HDDA suspensions for different HDDA concentrations (1 wt% PE).

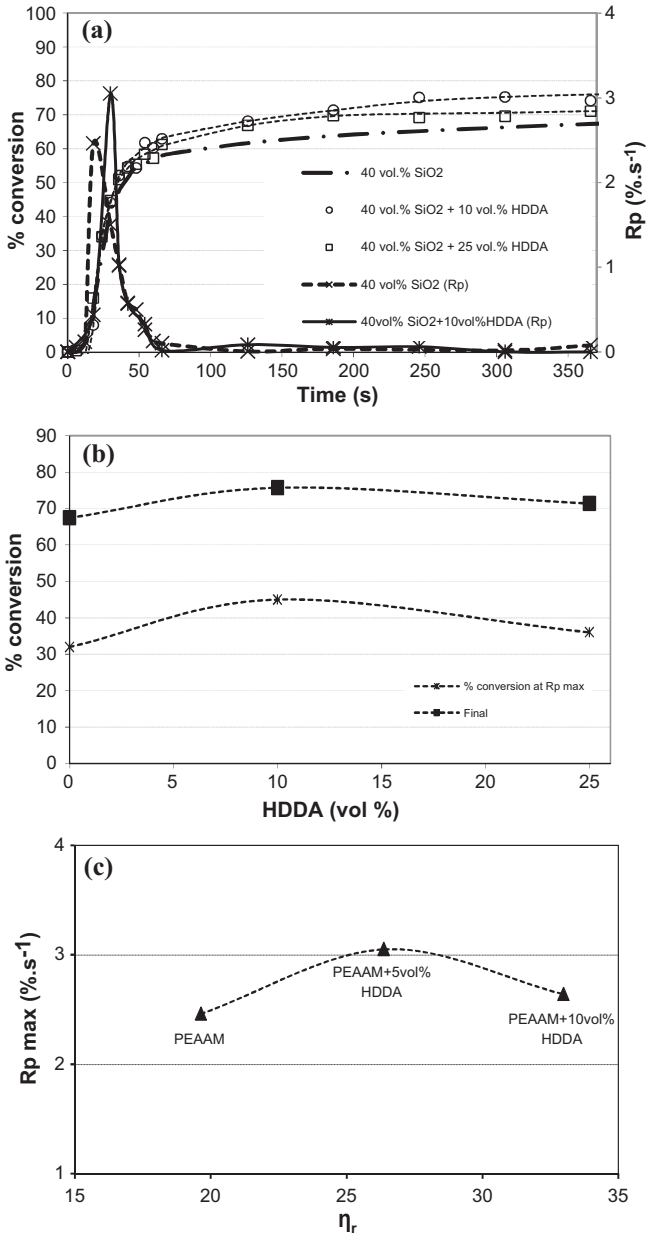

Fig. 11. Effect of HDDA addition on the photopolymerization of 40 vol% silica suspensions (1 wt% PE), under an energy doze of 5.3 mW cm^{-2}. (a) Conversion and polymerization rate versus time; (b) % conversion at maximum polymerization rate and at the end of the reaction, and (c) maximum polymerization rate versus relative viscosity.

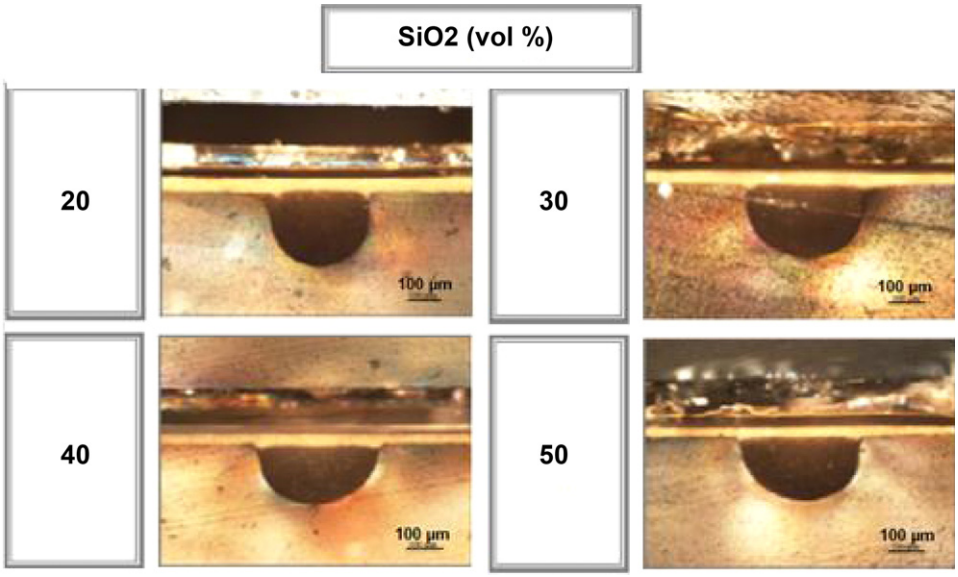

Fig. 12. Optical microscopy (10×) of polymerized line sections for different silica concentrations for an energy doze of 156 mJ cm^{-2} (1 wt% PE, 10 vol% HDDA).

considered as a pertinent indicator for the polymerization rate and for the conversion of the suspension during photopolymerization (Fig. 11c).

3.2. Stereolithography of silica suspensions: processing parameters

The key parameters in terms of UV reactivity of the suspension and of dimensional resolution are the polymerized thickness (E_p) and the polymerized width (L_p).[15–18] These two values were measured for silica suspensions with different powder concentrations (5–50 vol%) and containing 1 wt% of dispersant (with respect to the dry silica powder) and 10 vol% HDDA (with respect to the organic phase) (Fig. 12).

The contrast, due to the difference of index of refraction between the silica and the curable resin, even low, makes it possible to observe polymerized silica profiles (for silica concentrations above 20 vol%) which appear opaque.

The polymerized thickness is decreasing with the concentration of silica in the suspensions due to smaller penetration of the beam (D_p) caused by particle light scattering (Fig. 13a).[17–19]

The following Jacobs's equation shows that the polymerized width (L_p) is a function of the diameter of the laser spot ($2\omega_0$) and of the E_p/D_p ratio.

$$L_p = 2\omega_0\sqrt{\frac{E_p}{2D_p}} \tag{10}$$

It is verified that the polymerized width is increasing with the silica concentration in the suspensions (Fig. 13b).

For a given laser power, the density of energy (E_i) is a function of the laser scanning speed (Eq. (2)). In order to evaluate the influence of E_i on the polymerized thickness (E_p), seven scanning speeds were tested corresponding to delivered density of energy varying from 78 to 3591 mJ cm^{-2}. For all powder

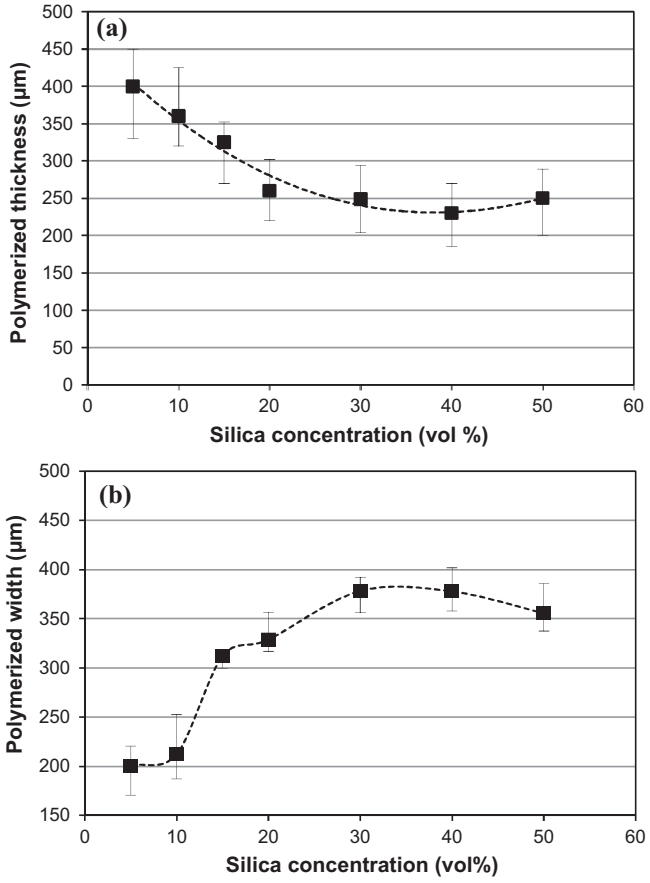

Fig. 13. Variation of the polymerized (a) thickness (E_p) and (b) width (L_p) with the silica concentration (1 wt% PE, 10 vol% HDDA, E_i = 156 mJ cm^{-2}).

concentrations, the polymerized thickness is linearly varying with ln(E_i) (Fig. 14), according to the Beer–Lambert law:

$$E_p = D_p \ln\left(\frac{E_i}{E_c}\right) \tag{11}$$

Table 4
Critical energy (E_c) and depth of penetration of the beam (D_p) values for silica suspensions with different powder loadings (1 wt% PE).

Ceramic	Powder loading (vol%)	D_p (μm)	σ^a (D_p)	E_c (mJ cm^{-2})	σ^a (E_c)
SiO_2	5	297	23	42	7
d_{50} = 2.25 μm	10	267	19	38	6
	15	250	15	39	7
	20	185	16	33	6
	30	137	5	23	9
	40	110	7	18	8
	50	99	7	5	8

[a] Standard deviation.

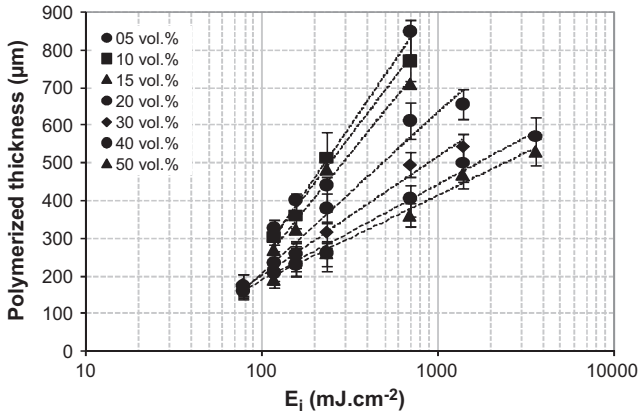

Fig. 14. Variation of the polymerized thickness in silica suspensions as a function of the delivered energy doze for different powder loadings (1 wt% PE).

E_c is the critical energy for photopolymerization, which is the minimum input energy necessary to trigger the curing process.[20]

Then, D_p and E_c parameters can be deduced respectively from the slope and intercept with the E_p axis (Fig. 14), and are reported in Table 4.

The critical energy is decreasing with silica concentration. This behavior was already reported by Hinczewski et al.[16] on alumina suspensions prepared with a similar curable system. By substituting the curable resin by inert ceramic particles, the surface energy necessary to the polymerization is decreasing. For low powder concentrations (<15 vol%; E_c = 39 mJ cm^{-2}), the value of E_c is close to that of the resin alone (i.e. 32 mJ cm^{-2}). For larger concentrations of ceramic powder (>15 vol%), that corresponds to a larger surface occupied by inert particles, the surface energy E_c necessary to initiate the photopolymerization process is decreasing down to 5 mJ cm^{-2} for 50 vol% silica.

4. Conclusion

The reaction of photopolymerization is essentially controlled by diffusion mechanisms of the various species involving in the propagation reaction (mobility of the reactive species) and in the termination reaction (mobility of radical sites developing the network). In this respect, the viscosity of a loaded system, and its evolution during polymerization, will directly influence the kinetics of polymerization and the conversion profile of the resin.

The evaluation of the respective contributions (i) of the rheology of suspensions containing ceramic particles, by means of the powder loading and the addition of dispersant and, (ii) of the rheology of the intergranular reactive phase, by means of the addition of diluent, on the photopolymerization, has demonstrated that for low concentrated mediums, the rheology of the loaded suspension (silica in this case) does not affect the photopolymerization in the concentration range tested (i.e. up to 10 vol%). The mobility of reactive functions, and then the polymerization kinetics, is only influenced by the intergranular phase. For highly concentrated systems, it is necessary to consider the particle–particle and particle–monomer interactions that limit the diffusion of free radicals in the medium, which results in a lowering of the degree of conversion as well as the polymerization rate of the resin.

The reactivity to UV of the suspension and the dimensional accuracy of the green part are critical parameters to control in this process. In one hand, the polymerized thickness (E_p), which is directly linked to the reactivity, is decreasing with the concentration of ceramic powder in the suspension due to particle light scattering. The evolution of the polymerized thickness, with respect to the density of energy, is in agreement with the Beer–Lambert law. In another hand, the polymerized width (L_p), which represents the dimensional resolution, is increasing with the powder concentration.

References

1. Chartier T, Chaput C, Doreau F, Loiseau M. Stereolithography of structural complex ceramic parts. *J Matter Sci* 2002;**37**(15):3141–7.
2. Brady GA, Halloran JW. Stereolithography of ceramic suspensions. *Rapid Prototyp J* 1997;**3**(2):61–6.
3. Griffith ML, Halloran W. Freeform fabrication of ceramics via stereolithography. *J Am Ceram Soc* 1996;**79**(10):2601–8.
4. Jacobs PF. *Rapid prototyping and manufacturing: fundamentals of stereolithography*. TX: Mc Graw Hill; 1993.
5. Chartier T, Duterte C, Delhote N, Baillargeat D, Verdeyme S, Delage C, et al. Fabrication of millimeter wave components via ceramic stereo- and microstereo-lithographie processes. *J Am Ceram Soc* 2008;**91**(8):2469–74.
6. Khalil H, Bila S, Aubourg M, Baillargeat D, Verdeyme S, Jouve F, et al. Shape optimized design of microwave dielectric resonators by level-set and topology gradient methods. *Int J RF Microw Comput Aided Eng* 2010;**20**:33–41.
7. Khalil H, Bila S, Aubourg M, Baillargeat D, Verdeyme S, Jouve F, et al. Shape optimization of a dielectric resonator for improving its unloaded quality factor. *Int J RF Microw Comput Aided Eng* 2011;**21**:120–6.
8. Chaput C, Delage C. 3D net-shape manufacturing of complex ceramic parts by high resolution stereo lithography – examples of application to

biomedical and industrial products. In: *7th international conference and exhibition on ceramic interconnect and ceramic microsystems technologies (CICMT 2011) proceedings*. 2011.
9. Halloran JW, Tomeckova V, Gentry S, Das S, Cilino P, Yuan D, et al. Photopolymerization of powder suspensions for shaping ceramics. *J Eur Ceram Soc* 2011;**31**(November (14)):2613–9.
10. Lecamp L, Youssef B, Bunel C, Lebaudy P. Photoinitiated polymerization of a dimethacrylate oligomer: 1. Influence of photoinitiator concentration, temperature and light intensity. *Polymer* 1997;**38**(25):6089–96.
11. Decker C, Moussa K. A new method for monitoring ultra-fast photopolymerizations by real-time infrared (RTIR) spectroscopy. *Makromol Chem* 1988;**189**:2381–94.
12. Decker C, Elzaouk B, Decker D. Kinetic study of ultrafast photopolymerization reactions. *J Macromol Sci Appl Chem* 1996;**3**(2):173–90.
13. Lecamp L. Photopolymérisation radicalaire de films de diméthacrylate: Etude cinétique et transposition à un système épais. PhD Thesis, INSA Rouen; 1997.
14. Wu KC, Halloran JW. Photopolymerization monitoring of ceramic stereolithography resins by RTIR methods. *J Mater Sci* 2005;**40**(1): 71–6.
15. Liao H, Coyle TW. Photoactive suspensions for stereolithography of ceramics. *J Can Ceram Soc* 1996;**65**(4):254–62.
16. Hinczewski C, Corbel S, Chartier T. Ceramic suspensions suitable for stereolithography. *J Eur Ceram Soc* 1998;**18**(6):583–90.
17. Aboulatim Y, Chartier T, Abelard P, Chaput C, Delage C. Optical characterization of stereolithography alumina suspensions using the Kubelka–Munk model. *J Eur Ceram Soc* 2009;**29**(5):919–24.
18. Tomeckova V, Halloran JW. Predictive models for the polymerization of ceramic suspensions. *J Eur Ceram Soc* 2010;**30**(14):2833–40.
19. Griffith ML, Halloran JW. Scattering of ultraviolet radiation in turbid suspensions. *J Appl Phys* 1997;**81**(6):2538–46.
20. Tomeckova V, Halloran JW. Critical energy for photopolymerization of ceramic suspensions in acrylate monomers. *J Eur Ceram Soc* 2010;**30**(16):3273–82.